Received: 4 August 2020 | Revised: 23 November 2020 | Accepted: 28 November 2020

DOI: 10.1002/jbm.b.34776

ORIGINAL RESEARCH REPORT

Society For Biomaterials | WILEY

Alumina-toughened zirconia for dental applications: Physicochemical, mechanical, optical, and residual stress characterization after artificial aging

Edmara T. P. Bergamo[1] | Karina B. Cardoso[1] | Lucas F. O. Lino[1] | Tiago M. B. Campos[2] | Kelli N. Monteiro[3] | Paulo F. Cesar[3] | Luis A. Genova[4] | Gilmar P. Thim[2] | Paulo G. Coelho[5] | Estevam A. Bonfante[1]

[1]Department of Prosthodontics and Periodontology, Bauru School of Dentistry – University of São Paulo, Bauru, SP, Brazil

[2]Department of Physics, Aeronautics Technological Institute, São José dos Campos, SP, Brazil

[3]Department of Biomaterials and Oral Biology, University of São Paulo, School of Dentistry, São Paulo, SP, Brazil

[4]Center of Materials Science and Technology, Institute of Research in Nuclear Energy, São Paulo, SP, Brazil

[5]Department of Biomaterials and Biomimetics, Hansjörg Wyss Department of Plastic Surgery, Mechanical and Aerospace Engineering, New York University, New York City, NY

Correspondence
Edmara T. P. Bergamo, Department of Prosthodontics and Periodontology, Bauru School of Dentistry – University of São Paulo, Al. Otávio Pinheiro Brisola 9-75, Bauru 17.012-901, SP, Brazil.
Email: edmaratatiely@gmail.com

Funding information
Fundação de Amparo a Pesquisa do Estado de São Paulo (FAPESP) Young Investigators, Grant/Award Numbers: 2012/19078-7, EMU 2016/18818-8, FAPESP 2019/08693-1, FAPESP 2018/19094-9; Conselho Nacional de Desenvolvimento Científico e Tecnológico (CNPq), Grant/Award Numbers: 304589/2017-9, 434487/2018-0; CAPES Finance Code, Grant/Award Number: 001

Abstract

To characterize the physicomechanical properties of an alumina-toughened zirconia (ATZ). ATZ synthesis consisted of the addition of alumina particles in an yttria-stabilized tetragonal zirconia polycrystals (3Y-TZP) matrix. Specimens were obtained by uniaxial and isostatic pressing ATZ and 3Y-TZP powders and sintering at 1600°C/1 h and 1550°C/1 h, respectively. Crystalline content and residual stress were evaluated using X-ray diffraction (XRD). Microstructure was characterized by scanning electron microscopy (SEM). Optical properties were determined by reflectance test. Mechanical properties were assessed by biaxial flexural strength test. All analyses were performed before and after aging (134°C, 20 h, 2 bar). XRD and SEM revealed a typical ATZ and 3Y-TZP crystalline content, chiefly tetragonal phase, with a dense polycrystalline matrix, though a smaller grain size for ATZ. Aging triggered a similar monoclinic transformation for both systems; however, ATZ exhibited higher residual compressive stresses than 3Y-TZP. While as-processed 3Y-TZP demonstrated significantly higher characteristic strength relative to ATZ, no significant difference was observed after aging (~215 MPa increase in the ATZ strength). ATZ presented significantly higher opacity relative to 3Y-TZP, although aging significantly increased the translucency of both systems (increase difference significantly higher in the 3Y-TZP compared to ATZ). ATZ physicomechanical properties support its applicability in the dental field, with a lower detrimental effect of aging relative to 3Y-TZP.

KEYWORDS
aging, ceramic composite, ceramics, mechanical properties, optical properties, zirconia

1 | INTRODUCTION

Zirconia is a polymorph material occurring in three distinct temperature-dependent crystallographic arrangements: cubic (*c*, 2370–2680°C), tetragonal (*t*, 1170–2370°C), and monoclinic (*m*, 1170°C after cooling to room temperature).[1] The development of zirconia as an engineering ceramic system has consisted of a polycrystalline tetragonal matrix stabilized at room temperature with the addition of 2–3 mol% yttrium oxide, named as yttria-stabilized tetragonal zirconia polycrystal (3Y-TZP).[2,3] The *t* phase remains metastable at room temperature and can revert to the most-stable *m* polymorph in a martensitic transformation when submitted to tensile stresses. Such

a *t-m* transformation is accompanied by a volumetric expansion of ~5% and shear strain of ~7%, inducing compressive stresses that can potentially act in opposition to the stress field that promotes crack propagation, thus increasing the fracture toughness of the material.[1,4] In fact, 3Y-TZP systems have the highest mechanical properties among currently available all ceramic systems, which along with the outstanding biocompatibility, have encouraged its use in the manufacturing of implants and prosthetic components that are indicated in a wide spectrum of load-bearing tissue reconstructions.[5-17] Despite promising survival rates for dental implants (95% after 1–5 years),[13,17] implant abutments (>97% after 5 years),[14,16] and dental prostheses (>90% after 5 years),[5-10] some reports have advised caution with the widespread use of 3Y-TZP systems, which can be more prone to fracture relative to their metallic counterparts.[5,10,12,15-17]

The technical concerns reported for 3Y-TZP reconstructions raise the question of its susceptibility to *t-m* phase transformation triggered by water presence at low temperatures, namely low temperature degradation (LTD).[18,19] Both effects, transformation toughening and LTD, arise from the polymorphic *t-m* transformation; however, spontaneous and progressive transformation by the exposure of 3Y-TZP systems to hydrothermal environments, eventually result in the elimination of any toughening effect.[20-22] LTD has shown to occur by diffusion of water species, initially located on oxygen vacancy sites due to the yttria doping, which lead to contraction of lattice parameters and accumulation of tensile stresses in the tetragonal grains, triggering *t-m* transformation.[18,19,23] Then, a cascade of *t-m* transformation might occur from the surface into the bulk of the material by a nucleation-and-growth process, which has shown to lead to surface roughening, eventually grain pull-out and microcracking, while deteriorate the density, mechanical properties and wear resistance of the 3Y-TZP.[18,20-24]A progressive *t-m* phase transformation has also been associated with an increase in the 3Y-TZP translucency, which may alter esthetic results of dental prostheses in the short-term.[20,24,25]

Based on such premises, several alternatives have been proposed to increase 3Y-TZP resistance to LTD, including the addition of a secondary crystalline phase to constrain *t-m* progression, that is, alumina that is biocompatible and presents satisfactory strength and toughness, high hardness and wear resistance.[20,22,24,26-28] Alumina-toughened zirconia (ATZ) ceramic composites are comprised of a disperse phase of alumina (α-Al_2O_3) in a zirconia matrix (3Y-TZP), targeting to bring together the advantageous properties of both ceramics as a result of a trade-off between enhanced toughening by crack-shielding and LTD resistance.[26-28] Previous studies have shown that the presence of uniformly dispersed α-Al_2O_3 particles limits the interconnectivity of zirconia grains, as well as its greater elastic modulus constrains 3Y-TZP grains in the ceramic matrix impeding an extensive *t-m* transformation and decreasing LTD phenomenon.[26-28] ATZ in different weight ratios of α-Al_2O_3 (10–20%) have previously demonstrated very promising reliability and lifetime relative to conventional 3Y-TZP, with no significant differences on the flexural strength, even after hydrothermal aging.[26-28] Particularly for restorative purposes, the presence of a secondary crystalline content has been associated with a detrimental effect on the light transmission of ceramic systems; however, their aging-resistant behavior may represent an advantageous feature for optical properties maintenance as *t-m* transformation has shown to increase 3Y-TZP translucency.[20,24,25] There is currently no study investigating the optical properties of ATZ ceramic composites; thus, research is warranted to comprehensively characterize ATZ physicomechanical properties and its aging stability.

The current study aimed to characterize the crystalline content and microstructure, and to evaluate the optical and mechanical properties of an experimentally processed ATZ ceramic composite in the weight ratio of 20% alumina and 80% 3Y-TZP before and after autoclave aging, for comparison with its isolated zirconia counterpart, 3Y-TZP. The postulated null hypotheses were that (a) ATZ would not demonstrate different optical properties parameters relative to 3Y-TZP before and after aging, and (b) ATZ would not demonstrate different flexural strength relative to 3Y-TZP before and after aging.

2 | MATERIALS AND METHODS

2.1 | Specimen preparation

A ceramic composite system, ATZ (TZ-3YS20AB, Tosoh corporation, Tokyo, Japan), comprised of 80% first-generation zirconia, 3 mol% yttria-stabilized tetragonal zirconia polycrystal (3Y-TZP), and 20% high-purity alfa alumina (α-Al_2O_3) was characterized in the current study, for comparison with the isolated zirconia counterpart, 3Y-TZP (TZ-3YSB-E, Tosoh). The composition and particle size of the two commercial powders are given in the Table 1.

Disc-shaped specimens were produced through uniaxially pressing the ceramic powder at a pressure of 1148 kgf/cm^2 for 30 s in a tungsten carbide matrix of 18 mm diameter and 1.8 mm thickness to compensate for sintering shrinkage. Green body discs were double wrapped and sealed in vacuum sealer (Jumbo Plus, Globavac, Itajai, SC, Brazil) and subjected to isostatic pressing (National Forge, Irvine, PA) at 2110 kgf/cm^2 for 30 s at room temperature. Then, green body samples of ATZ and 3Y-TZP were sintered at 1600 and 1550°C for 1 hr in a furnace (Ivoclar Vivadent AG, Schaan/Liechtenstein, Austria) with heating and cooling rate of 4°C/min. The 3Y-TZP sintering protocol was based on previous studies of the current group, where a dense microstructure with high optical and mechanical properties were obtained.[20,24] In contrast, the sintering protocol for the ATZ

TABLE 1 Composition and particle size of the ATZ and 3-TZP powders used in the study

	Powders chemical composition (wt%)				
Material	Y_2O_3	Al_2O_3	Na_2O	SiO_2	FeO_2O_3
ATZ	4.2	20.08	11	≤0.002	≤0.002
3Y-TZP	5.2	≤0.1 ~ 0.4	≤0.04	≤0.002	≤ 0.01

Abbreviations: 3Y-TZP, yttria-stabilized tetragonal zirconia polycrystals; ATZ, alumina-toughened zirconia.

ceramic composite was established based on the results of a pilot test, where four different sintering protocols were investigated: (a) 1500°C for 2 h, (b) 1550°C for 1 hr, (c) 1550°C for 2 hr, and (d) 1600°C for 1 hr. X-ray diffraction (XRD) and scanning electron microscopy (SEM) were used to evaluate the crystalline content and microstructure, as well as biaxial flexural strength (BFS) test to investigate strength differences of the proposed protocols (n = 10/protocol), as per methodologies described below in detail. The results indicated typical zirconia and alumina peaks and a dense microstructure for all protocols, where a grain size increase was observed as sintering temperature and time increased (Figure 1); however sintering at 1600°C for 1 hr resulted in higher BFS (1156 ± 116 MPa), followed by 1550°C for 2 hr (1014 ± 237 MPa), 1500°C for 2 hr (947 ± 149 MPa), and 1550°C for 1 hr (870 ± 218 MPa).

After sintering all specimens, a mirror-like finish polishing was performed in a semiautomatic polishing machine (Automet 2000, Buehler, Lake Buff, IL) with 220, 120, 90, 40, 25, and 9 μm granulated diamond disks (ALLIED High Tech Products, Rancho Dominguez, CA) and 6, 3, and 1 μm diamond suspensions until a final dimension of 1 mm thickness (14 × 1 mm/ISO 6872:2015). A total of 90 discs for each experimental group, ATZ and 3Y-TZP, were prepared for XRD, SEM, reflectance tests in a spectrophotometer, and BFS testing.

The characterization tests were performed before and after artificial aging using autoclave (Vitale Class CD 12 L, Cristófoli, Campo Mourão, PR, Brazil) to induce tetragonal-to-monoclinic (t-m) phase transformation. An evidence-based protocol for 3Y-TZP aging of 134°C, for 20 hr at 2 bar, which has previously shown to affect its optical and mechanical properties,[20,24,29] was used to simulate a challenging clinical situation to compare the ceramic systems aging resistance.

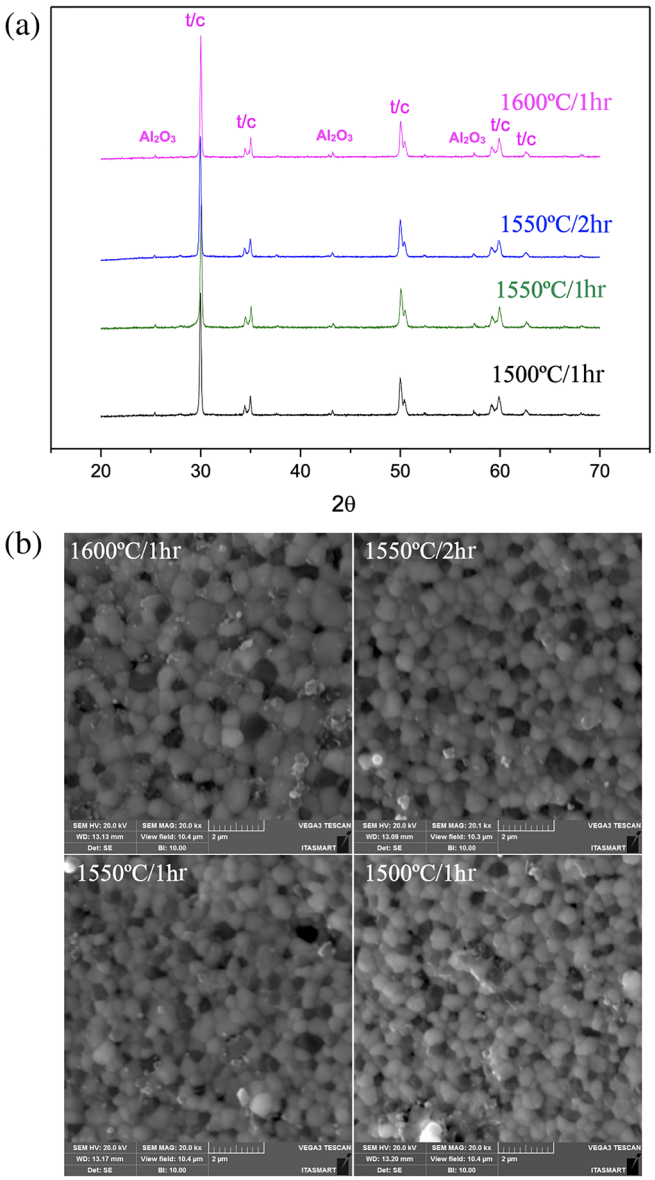

FIGURE 1 X-ray diffraction spectra (a) and scanning electron micrographs (b) of ATZ system sintered at different protocols

2.2 | X-ray diffraction

Crystalline spectra were obtained by XRD (Miniflex, Rigaku, Tokyo, Japan). Standard incidence XRD scanning was performed on the Bragg θ-2θ geometry, equipped with a graphite monochromator and Cu Kα radiation (λ = 1.5406 Å), operating at a voltage of 40 kV and a current emission of 40 mA. The data were obtained over a 2θ range of 20–70° at a scan rate of 0.2°/min and a step size of 0.020°. Characteristic zirconia peaks were identified using JCPDS-ICDD (file 81–1545). Quantitative phase analysis was carried out using the formulas introduced by Toraya and Yoshimura.[30]

The residual stress was also determined by means of XRD, with the same equipment described above, where the scanning was performed on the Bragg θ-2θ geometry ranging from 90 to 100° at 10 s per scan step, as detailed elsewhere.[31,32] The peak displacement was analyzed at 95°, which was determined considering the value of 2θ corresponding to the center of the peak.

2.3 | Scanning electron microscopy

The micromorphology obtained by the different sintering protocols tested in the pilot study was analyzed by SEM (VEGA3-TESCAN, Brno-Kohoutovice, Czech Republic). The field-emission gun scanning electron microscope (FEG-SEM, MIRA3-TESCAN, Brno-Kohoutovice, Czech Republic) was used for final characterization of the microstructure and ceramic systems comparisons. SEM images were obtained using the secondary electron (SE) detector, at high vacuum, 5 kV accelerating voltage, and magnifications of 20,000 and 50,000×. The grain size was determined on the SEM images using the mean equivalent circle diameter method (ISO 133383-1:2012).

2.4 | Optical properties

The contrast ratio (CR) and translucency parameter (TP) by color difference (ΔE) measurements were determined using parameters

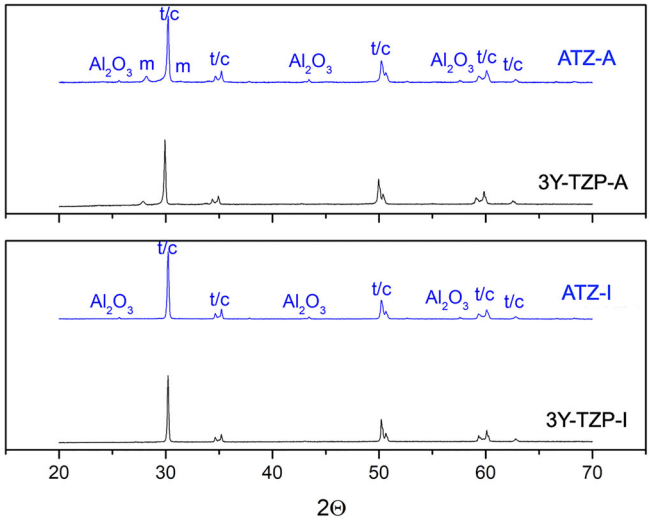

FIGURE 2 X-ray diffraction spectra of alumina-toughened zirconia (ATZ) and 3Y-TZP before and after aging, where the scanning was performed on the 2θ ranging from 20 to 70°

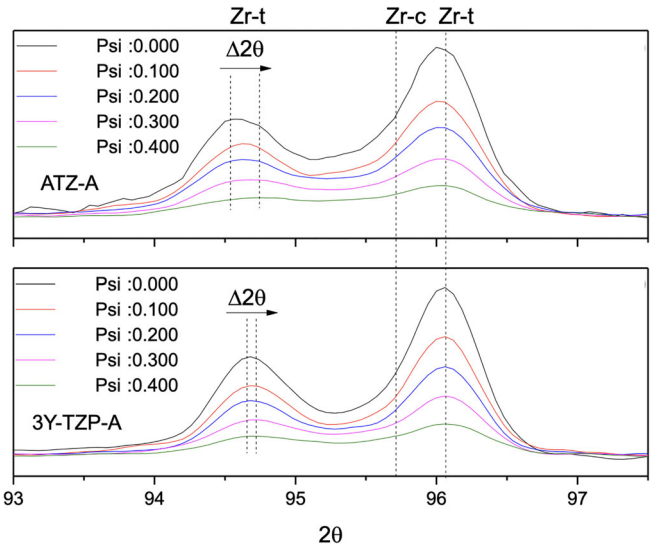

FIGURE 3 X-ray diffraction spectra of the aged samples for different incidence angle (Psi), ranging from 0.000 to 0.400, where the scanning was performed on the 2θ ranging from 90 to 100°

obtained by reflectance tests performed with a bench top spectrophotometer (CM 3700d Konica Minolta, Tokyo, Japan). The specimens were placed on a black (b) and white (w) backgrounds cards for determining the reflectance values and CIE L*a*b* color coordinates with a wavelength of 400–700 nm (within visible light range) to consider the reflectivity of a sheet having no reflective background (black) and that of a sheet having a reflective background.[20,24,33]

CR is the property that measures the transparency or opacity of the material and is measured by the ratio of reflectance of the specimen on the black background (Yb) to the reflectance of the same specimen on a white background (Yw), which is given by: $CR = Yb/Yw$.

TP, which defines the masking ability of the material, was obtained by calculating the color difference (ΔE) of the specimens on the black and white backgrounds, according to the formula: $\Delta E = \left[\left(L_b^* - L_w^*\right)^2 + \left(a_b^* - a_w^*\right)^2 + \left(b_b^* - b_w^*\right)^2\right]^{1/2}$ where, the subscripts b* (black) and w* (white) indicate the background color, and the coordinates L*, a*, and b* correspond to the lightness, chromaticity on the red/green axis, and chromaticity on the yellow/blue axis, respectively. The test was performed in the same sample before and after aging (n = 10/material).

2.5 | Biaxial flexural strength

BFS test was performed using a piston-on-three balls device, according to ISO 6872:2015 on a servo all-electric equipment (ElectroPulsTM E3000 Linear-Torsion, Instron, Norwood, MA, EUA). The discs-shaped specimens were positioned on the three-ball support, which were placed 11-mm equidistant from each other in a triangular position. The tests were performed at room temperature, with a flat circular piston attached to a load cell of 500 Kgf applying a load at a crosshead speed of 0.5 mm/min in the center of the specimen until failure. The maximum load was recorded (N), and the following equations were used to calculate BFS (MPa):

$$\sigma = -0.2387\,P(X-Y)/b^2, X = (1+\nu)Ln(r_2/r_3)^2 + (1[1-\nu]/2)(r_2/r_3)^2,$$
$$\text{and } Y = (1+\nu)(1+Ln[r_1/r_3])^2 + (1-\nu)(r_1/r_3)^2,$$

where σ is BFS (MPa), P the fractured load (N), b is the specimen thickness at fracture site (1.2 ± 0.2 mm), v is the Poisson ratio (0.25), r_1 the radius of support circle (5.5 mm), r_2 the radius of loaded area (0.75 mm), and r_3 is the radius of the specimen (7 mm).

The fractured specimens were examined in the Axio Zoom V16 Stereo Zoom Microscope (Zeiss, Oberkochen, Germany) to assess fractographic marks evidence of the fracture origin and direction of propagation.

2.6 | Statistical analysis

Data from optical properties (CR and TP) were tabulated and subjected to descriptive analysis, normality and homoscedasticity tests. Data normality and homoscedasticity were confirmed using Shapiro–Wilk ($p > 0.05$) and Levene ($p > 0.25$) tests, respectively. Hence, data were statistically evaluated using repeated-measure analysis of variance following post-hoc comparisons by Tukey test, at a significance level of 5% using SPSS software (IBM SPSS Statistics version 27, Armonk, NY). Data are presented as a function of the estimated mean and 95% confidence interval (CI).

BFS stress data (MPa) were analyzed using Weibull 2-parameter statistical analysis (Synthesis 9, Weibull ++9, Reliasoft, Tucson, AZ). Use level probability Weibull curves were calculated and plotted along with the corresponding 90% CI. Also, characteristic stress (MPa) and Weibull modulus (m) were calculated and a contour plot was graphed to determine statistical differences between groups (90% CI). In addition, the probability of survival (1-probability of failure, P_f) and the

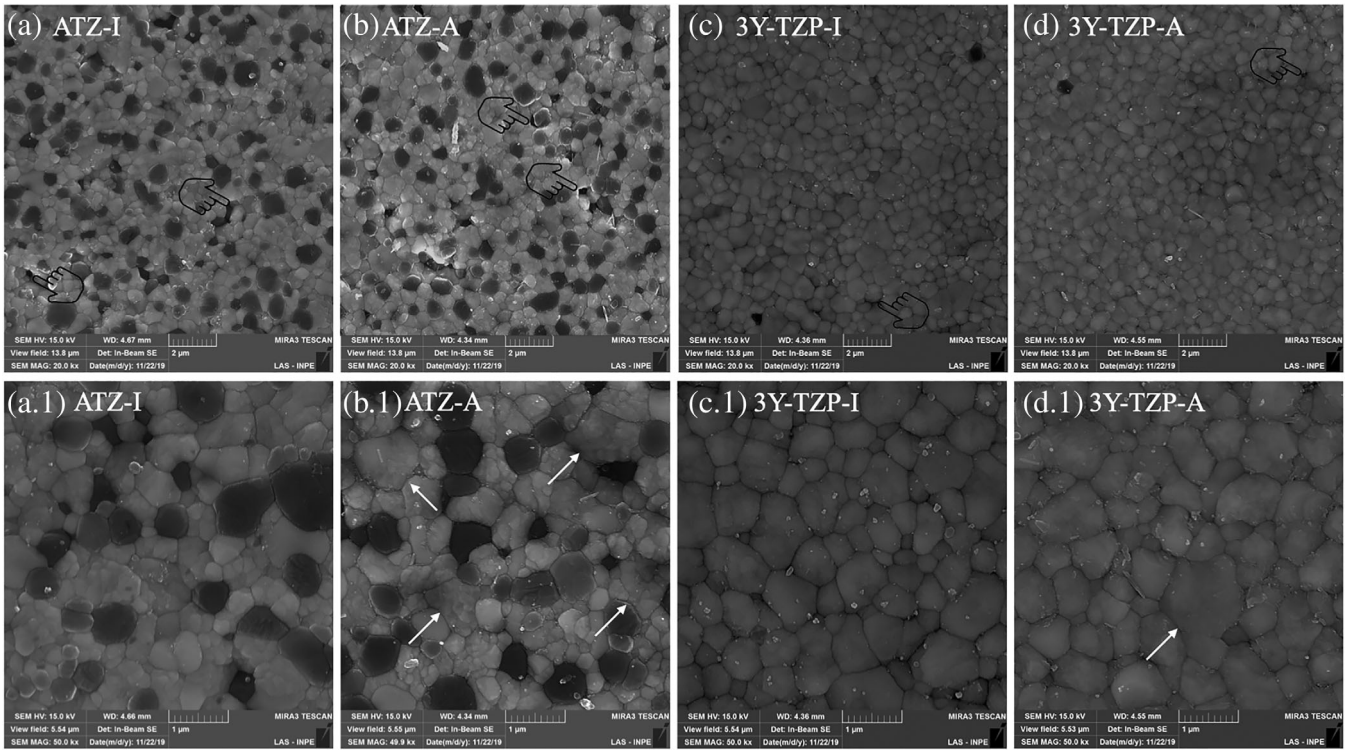

FIGURE 4 Scanning electron micrographs of immediate and aged alumina-toughened zirconia (ATZ) and 3Y-TZP at 20,000× (a–d) and 50,000× (a.1–d.1) magnifications. The arrows show the volumetric grain increase caused by phase transformation, especially in the ATZ system; moreover, the pointers indicate microstructural defects originated from ceramic processing and/or aging

TABLE 2 Contrast ratio (CR) and translucency parameter (TP) mean values with respective 95% confidence interval (IC) values

		Contrast ratio	Translucency parameter
ATZ	Immediate	0.99 (0.002) A	0.21 (0.081) D
	Aged	0.96 (0.023) B	1.41 (0.956) C
3Y-TZP	Immediate	0.85 (0.003) C	7.12 (0.096) B
	Aged	0.79 (0.028) D	10.0 (1.143) A

Note: Different letters indicate statistically significant difference.
Abbreviations: 3Y-TZP, yttria-stabilized tetragonal zirconia polycrystals; ATZ, alumina-toughened zirconia.

respective 90% CI as a function of stress values at fracture were calculated to predetermined service stresses of 100, 300, and 500 MPa. The following equation and derivatives were used in the software analyses, as described in the ISO 6872:2015: $P_f = exp\left\{-\left(\frac{\sigma}{\sigma_0}\right)^m\right\}$.

3 | RESULTS

XRD spectra analysis allowed the identification of typical alumina and zirconia crystalline peaks, where a low intensity α-alumina peak can be observed in the ATZ, given its small weight percentage (20%). No significant monoclinic content was observed in the as-processed ceramic systems, ATZ and zirconia, indicating that both sintering protocols provided a predominant crystallization of zirconia tetragonal phase, yttria-stabilized tetragonal zirconia polycrystal system, 3Y-TZP. Artificial aging triggered a similar tetragonal-to-monoclinic (*t-m*) phase transformation for both polycrystalline ceramics, ATZ and 3Y-TZP, with approximately 12.3% monoclinic content in the former and 13.2% in the latter (Figure 2).

XRD spectra of the aged ATZ and 3Y-TZP for the different incidence angle (Psi) depict the tetragonal zirconia peak at 2θ approximately 94.7° and an overlap of the tetragonal and cubic zirconia peaks at 2θ approximately 96°. 3Y-TZP tetragonal peak at 94.7° had a smaller displacement as a function of Psi relative to ATZ, which showed a comparatively larger shift as the Psi increased. As beam penetration is inversely proportional to Psi, more compressive stresses as a consequence of degradation process and volumetric increase of grains caused by phase transformation were present at the external surface of ATZ disc relative to 3Y-TZP (Figure 3). In addition, the calculated residual stress for aged ATZ, based on the elastic strain, which can be measured from the varying interplanar distances, and the elastic modulus of the material, was −488 ± 40 MPa, whereas 3Y-TZP residual stress was −37 ± 12 MPa. The as-processed ceramic systems did not present any detectable residual stresses and thus were not included in the current analysis.

SEM images of the ATZ and 3Y-TZP systems showed a dense fully crystalline ceramic matrix for both systems, with the presence of spherical grains and few intergranular defects on the surface that may be related to the processing protocol. Moreover, a uniform arrangement of the alumina grains in the 3Y-TZP matrix can be observed in

the ATZ ceramic composite, without the presence of agglomerates. Smaller grain size can be observed for the nonaged ATZ (0.392 ± 0.212 μm) relative to 3Y-TZP (0.565 ± 0.208 μm), which may be related to the presence of alumina that leads to a reduction in the zirconia grain growth. While ATZ (0.566 ± 0.219 μm) exhibited a remarkable volumetric grain increase after aging, 3Y-TZP grain increase (0.560 ± 0.228 μm) was hardly observed. The size of alumina grains showed no meaningful difference between immediate (0.480 ± 0.194 μm) and aged ATZ (0.523 ± 0.203 μm) samples (Figure 4).

ATZ demonstrated significantly higher contrast ratio (CR, 0.99 ± 0.002) relative to its isolated zirconia counterpart, 3Y-TZP (0.85 ± 0.003) ($p < 0.001$). Laboratory aging significantly decreased the opacity of both polycrystalline ceramic systems (ATZ: 0.96 ± 0.023 and 3Y-TZP: 0.79 ± 0.028) ($p < 0.012$), with ATZ maintaining CR values significantly higher than 3Y-TZP ($p < 0.001$). Conversely, ATZ demonstrated significantly lower translucency parameter (TP, 0.21 ± 0.081) relative to its isolated zirconia counterpart, 3Y-TZP (7.12 ± 0.096) ($p < 0.001$). Laboratory aging significantly decreased the masking ability of both polycrystalline ceramic systems (ATZ: 1.41 ± 0.956 and 3Y-TZP: 10.0 ± 1.143) ($p < 0.018$), with ATZ maintaining TP values significantly lower than 3Y-TZP ($p < 0.001$) (Table 2).

3Y-TZP and ATZ showed no significant difference on the Weibull modulus (m) (ATZ: 8.24 and 3Y-TZP: 9.51), irrespective of aging condition, although both systems presented a decrease in the m values after aging (ATZ: 4.15 and 3Y-TZP: 6.49), statistically significant for the ATZ ceramic composite. Immediate 3Y-TZP demonstrated statistically higher characteristic strength (1215 MPa) relative to aged 3Y-TZP (1033 MPa) and ATZ, irrespective of storage condition. Although as-processed ATZ presented the lowest characteristic strength (744 MPa), it significantly increased after aging (962 MPa), with no significant difference when compared to aged 3Y-TZP, as indicated by the overlap between the contour plots (Figure 5 and Table 3).

At 100 and 300 MPa service stresses, which correspond to the ISO 6872:2015 indication for single crowns and 3-unit anterior (up to premolar) fixed dental prostheses (FDP), respectively, both ATZ and 3Y-TZP systems would result in a high probability of survival (approximately 99%). Although a statistically significant reduction in the probability of survival of ATZ at 500 MPa, required stress to 3-unit posterior FDP, the survival estimate would maintain values higher than 94%, irrespective of aging condition (Table 4).

Number of fractured fragments varied from two to five for both polycrystalline ceramic systems, irrespective of aging condition, with the most representative failure modes illustrated in the Figures 6 and 7. Fractographic marks, including hackle lines and compression curls, were used to diagnose the origin of the fracture, generally related to tensile side defects originated during processing and/or aging ceramic specimens, which propagated to the opposite compression side.

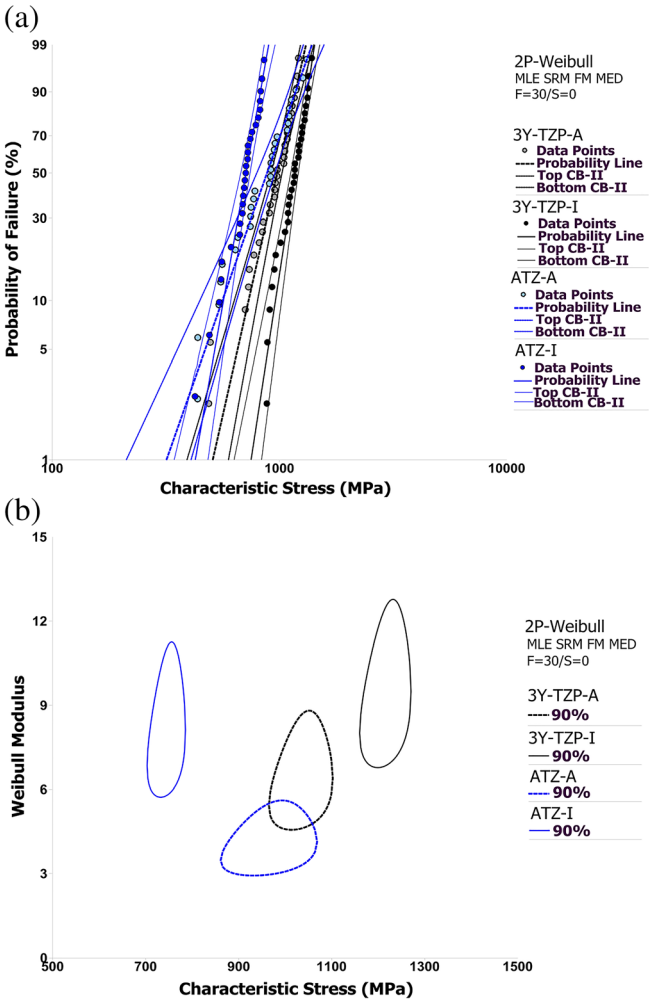

FIGURE 5 (a) Use level probability Weibull curves, showing the probability of failure as a function of characteristic stress (MPa). (b) Contour plot showing the relationship between Weibull modulus (m) and characteristic stress (MPa). The nonoverlap between contours indicates statistically significant difference

TABLE 3 Weibull modulus (m), and characteristic stress (MPa) with the corresponding 95% confidence interval

		Weibull modulus	Characteristic stress (MPa)
ATZ	Immediate	8.24 (6.37–10.65) A	744 (715–775) C
	Aged	4.15 (3.24–5.32) B	962 (889–1041) B
3Y-TZP	Immediate	9.51 (7.47–12.11) A	1215 (1175-1256) A
	Aged	6.49 (5.05–8.33) AB	1033 (984–1084) B

Note: Different letters indicate statistically significant difference.
Abbreviations: 3Y-TZP, yttria-stabilized tetragonal zirconia polycrystals; ATZ, alumina-toughened zirconia.

TABLE 4 Calculated reliability (%) with the corresponding 95% confidence interval at a set stress of 100, 300, and 500 MPa

		ATZ		3Y-TZP	
		Immediate	Aged	Immediate	Aged
100 MPa	Upper bound	100	100	100	100
	Reliability	100 aA	100 aA	100 aA	100 aA
	Lower bound	100	100	100	100
300 MPa	Upper bound	100	100	100	100
	Reliability	100 aA	99 aAB	100 aA	100 aA
	Lower bound	100	97	100	100
500 MPa	Upper bound	99	97	100	100
	Reliability	96 bB	94 bB	100 aA	99 abA
	Lower bound	90	86	100	97

Note: Different lowercase letters indicate statistical difference between materials and different conditions. Different uppercase letters indicate statistical difference between missions.
Abbreviations: 3Y-TZP, yttria-stabilized tetragonal zirconia polycrystals; ATZ, alumina-toughened zirconia.

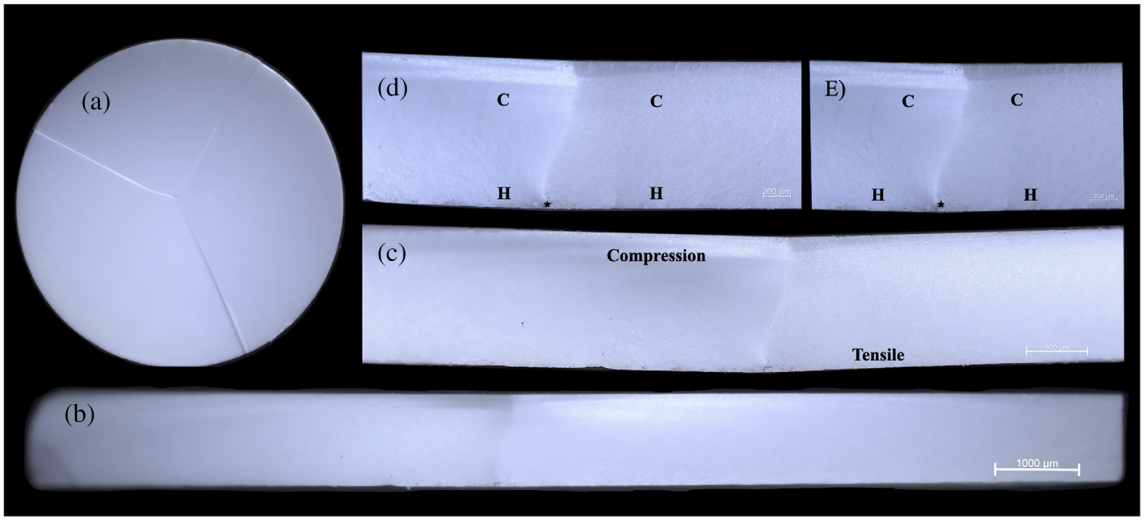

FIGURE 6 Polarized light stereomicrographs of a representative alumina-toughened zirconia (ATZ) sample fractured in three pieces, showing an overview (a,b) and higher magnifications (c–e) images. Previously observed marks are corroborated in the high magnification micrographs (d-e), where fracture initiation (asterisk) and direction of propagation, from the tensile side to the compression side (c), are indicated by fractographic marks, such as hackle lines (h) and compression curl (c)

4 | DISCUSSION

The current study characterized the optical and mechanical properties of an experimentally processed ATZ ceramic composite, 80% 3Y-TZP and 20% α-Al_2O_3, before and after artificial aging, for comparison with the results of its 3Y-TZP isolated counterpart. Based on data analyses, as-processed ATZ presented significantly higher opacity than 3Y-TZP, where an increased translucency was observed for both systems after aging, with the increase difference significantly higher in the 3Y-TZP compared to ATZ; thus, the first postulated null hypothesis that ATZ would not demonstrate different optical properties parameters relative to 3Y-TZP before and after aging was rejected. Although as-processed ATZ demonstrated significantly lower flexural strength relative to 3Y-TZP, an increased flexural strength was observed for ATZ after aging, similar to the aged 3Y-TZP that presented a significant reduction in the flexural strength; thus, the second postulated null hypothesis that ATZ would not demonstrate different flexural strength relative to 3Y-TZP before and after aging was also rejected.

The characterization tests revealed the success of the proposed processing method, where a typical α-Al_2O_3 and 3Y-TZP crystalline content, with a predominant tetragonal phase, as well as high-density polycrystalline ceramics were obtained for both systems. Besides, a uniform distribution of α-Al_2O_3 particles within the 3Y-TZP matrix was observed for the ATZ, which presented a smaller grain size relative to its isolated counterpart. The difference in the as-processed ceramics grain size may be related to the presence of α-Al_2O_3 crystals in the ceramic composite, which has previously shown to act as a dopant; consequently, controlling grain size and decreasing yttria content

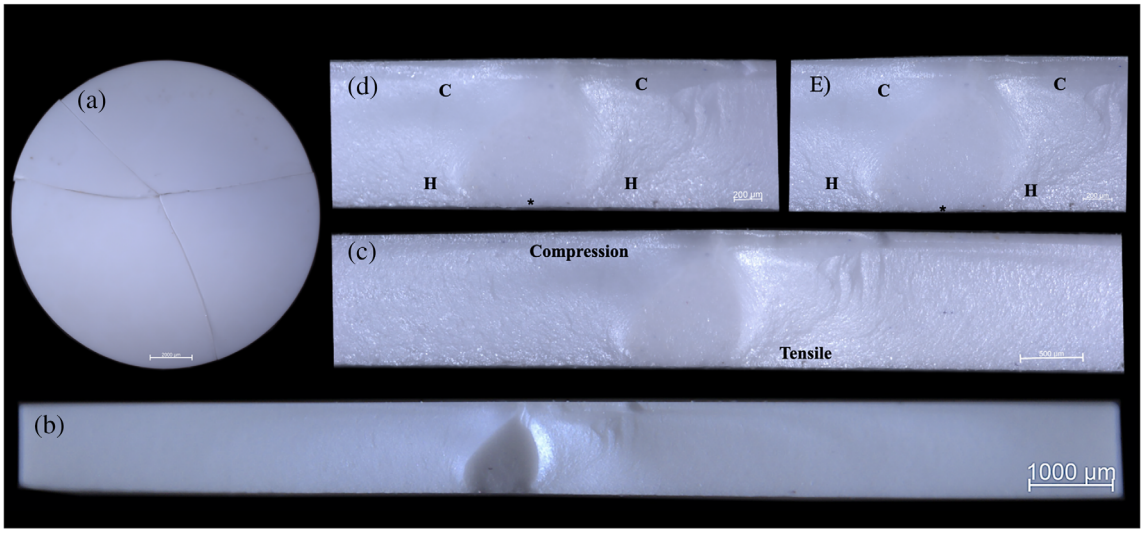

FIGURE 7 Polarized light stereomicrographs of a representative alumina-toughened zirconia (ATZ) sample fractured in four pieces, showing an overview (a,b) and higher magnifications (c–e) images. Previously observed marks are corroborated in high magnification micrographs (d-e), where fracture initiation (asterisk) and direction of propagation, from the tensile side to the compression side (c), are indicated by fractographic marks, such as hackle lines (h) and compression curl (c)

need in the ATZ formulation,[34] as observed in the current ceramic powder. Nonetheless, ceramics micromorphology and its preservation over time have shown to dictate the physicomechanical properties and reconstructions longevity.[5-17,20-24,26-28,31,35] 3Y-TZP metastability makes it susceptible to LTD phenomenon.[18,19] Given ATZ α-Al_2O_3 content and smaller grain size relative to 3Y-TZP, a slower aging process could be expected because of a lower trend to *t-m* transformation[26,35,36]; however, the observed *t-m* kinetics was similar for both ceramic systems with an increase in the amount of monoclinic content of approximately 12%. This behavior may lie on the invariably present exposition to hydrothermal stimuli and interconnectivity of zirconia grains, where the 20% α-Al_2O_3 content was not capable of restricting the nucleation of LTD.[27] Thus, different α-Al_2O_3 weight percentages, particle size or dopant type or combinations should be pursued to reach a more favorable balance between LTD resistance and toughening mechanisms in ATZ ceramic composites.

Both polycrystalline systems presented high opacity, which fosters clinical use in cases where darkened substrates such as titanium implant abutments or darkened teeth should be masked.[20,24] Several factors have been associated with the increased light scattering of polycrystalline systems, including the birefringent nature of noncubic crystals, grain size, presence of pores and flaws, and surface roughness, as well as a secondary crystalline content.[3,37-40] The precipitation of α-Al_2O_3 crystals drastically reduced the TP and increased the CR of the ATZ relative to its isolated zirconia counterpart, 3Y-TZP. Even with the use of a high sintering temperature (1600 and 1550°C for ATZ and 3Y-TZP, respectively), previously shown to increase the density of polycrystalline systems and reduce residual porosity thereby decreasing light scattering, no improvement in the ATZ translucency was observed.[3,41] Furthermore, autoclave aging significantly increased the translucency of both ceramic systems; however, the increase difference in the TP values were 1.67 higher in the 3Y-TZP than ATZ. Given the similar *t-m* transformation observed for both materials after laboratory aging, favoring light transmission as a consequence of the polycrystalline matrix rearrangement (including crystal phase, size and shape), as well as similar presence of pores and defects, the lower increase difference for the ATZ ceramic composite may indeed be related to impaired light transmission caused by the α-Al_2O_3 content.[38,39]

Although autoclave aging triggered a similar *t-m* transformation for both systems, ATZ exhibited higher residual compressive stresses than 3Y-TZP, which resulted in an increased flexural strength after aging (∼215 MPa increase), similar to the aged 3Y-TZP that showed a significant reduction in the flexural strength. The rationale for such differences may lie on the composition, crystalline content, microstructure, *t-m* transformation, and micromorphological changes after aging that increased residual compressive stresses presence in the ATZ ceramic composite.[26-28,31,35,36] Firstly, α-Al_2O_3 has a lower mechanical strength relative to 3Y-TZP, thus its presence in ceramic composites tends to proportionally decrease the flexural strength as the percentage of alumina increases.[27] Nonetheless, residual compressive stresses have shown to change the ceramic surface to the benefit of their strength.[28,31] Hence, the dense compressive layer resulting from the *t-m* transformation crystalline rearrangement, increased by alumina mechanical constriction (its higher stiffness enhances the energy threshold for *t-m* transformation in the vicinity grains), limited crack propagation and improved ATZ flexural strength after aging.[31,36] This fact may be related to the previously described superficial *t-m* transformation in ATZ, where the nucleation process has shown to occur due to zirconia grains exposition to hydrothermal stimuli while the growth rate of the *m* phase was decelerated due to the presence of α-Al_2O_3 particles.[26-28] Cross-sectional evaluations of

the in-depth *t-m* transformation profile confirm such assumptions.[27] Moreover, despite the similar *t-m* transformation, 3Y-TZP samples presented a reduced compressive layer, which more rapidly reached the critical stress necessary to initiate fracture and significantly reduced the characteristic strength relative to 3Y-TZP immediate samples. In fact, it has been previously shown that a critical transformation depth, resulting in a lower concentration of compressive stresses and increased defects/microcracks population, is required to decrease mechanical strength.[31,42] Hence, the current degradation protocol may have resulted in a deeper *m* phase occurrence in the 3Y-TZP, which may not have been detected in the XRD due to the limited beam penetration, inducing critical defects/microcracks appearance.[26,27,42] Therefore, the amount of strength improvement/degradation after hydrothermal aging is dependent on the composition and compressive layer density on the surface and, consequently, its blunting effect on the material defects.[35] Altogether, the use of ATZ ceramic composites may be clinically favorable due to a retard in the detrimental effect of the LTD on its mechanical properties, which may induce a longer benefit of toughening mechanisms (perhaps longer than the expected prosthesis lifetime).

The probability of survival for missions compatible with the indication of single crowns to 3-unit anterior and posterior FDP at 100, 300, and 500 MPa respectively (ISO 6872:2015), resulted in a high probability of survival (at least 94%) for both systems. Moreover, the percentage of *t-m* transformation (~12%) was below the fraction specified on international standards (ISO 13356:2008) for implants indication (25%). These predictions highlight the potential indication of ATZ systems in a range of applications, including dental implants where ATZ marketing is increasing.[43] Nonetheless, testing these materials for fatigue performance is paramount to comprehensively characterize their lifetime.

5 | CONCLUSIONS

Based on the limitations of an in vitro study, the following conclusions can be drawn:

1. ATZ ceramic composite exhibited similar monoclinic content relative to yttria-stabilized tetragonal zirconia polycrystals (3Y-TZP) before and after aging, simulating LTD; however, higher residual compressive stresses were observed for ATZ after aging;
2. While immediate ATZ showed significantly lower characteristic strength relative to 3Y-TZP, no significant difference was observed after aging, with ~215 MPa increase in the ATZ strength;
3. ATZ opacity is significantly higher than 3Y-TZP, though the increase in translucency after aging was significantly higher for the 3Y-TZP;
4. The physicochemical and mechanical properties of ATZ support its applicability in the dental field, with a lower detrimental effect of LTD relative to 3Y-TZP; however, additional innovations are required to further improve its immediate properties and hydrothermal stability.

DATA AVAILABILITY STATEMENT

Data will be provided upon request.

ORCID

Edmara T. P. Bergamo https://orcid.org/0000-0002-5006-2184
Estevam A. Bonfante https://orcid.org/0000-0001-6867-8350

REFERENCES

1. Garvie RC, Hannink RH, Pascoe RT. Ceramic steel? *Nature*. 1975;*258*:703-704.
2. Chevalier J, Gremillard L. Ceramics for medical applications: a picture for the next 20 years. *J Eur Ceram Soc*. 2009;*29*(7):1245-1255.
3. Zhang Y, Lawn BR. Novel zirconia materials in dentistry. *J Dent Res*. 2018;*97*(2):140-147.
4. Stevens R, Evans P. Transformation toughening by dispersed polycrystalline zirconia. *Trans J Br Ceram Soc*. 1984;*83*(1):28-31.
5. Pieralli S, Kohal RJ, Rabel K, von Stein-Lausnitz M, Vach K, Spies BC. Clinical outcomes of partial and full-arch all-ceramic implant-supported fixed dental prostheses. A systematic review and meta-analysis. *Clin Oral Implants Res*. 2018;*29*(18):224-236.
6. Pjetursson BE, Sailer I, Makarov NA, Zwahlen M, Thoma DS. Corrigendum to "all-ceramic or metal-ceramic tooth-supported fixed dental prostheses (FDPs)? A systematic review of the survival and complication rates. Part II: multiple-unit FDPs" [dental materials 31 (6) (2015) 624-639]. *Dent Mater*. 2017;*33*(1):e48-e51.
7. Pjetursson BE, Valente NA, Strasding M, Zwahlen M, Liu S, Sailer I. A systematic review of the survival and complication rates of zirconia-ceramic and metal-ceramic single crowns. *Clin Oral Implants Res*. 2018;*29*(16):199-214.
8. Rabel K, Spies BC, Pieralli S, Vach K, Kohal RJ. The clinical performance of all-ceramic implant-supported single crowns: a systematic review and meta-analysis. *Clin Oral Implants Res*. 2018;*29*(18):196-223.
9. Sailer I, Makarov NA, Thoma DS, Zwahlen M, Pjetursson BE. Corrigendum to "all-ceramic or metal-ceramic tooth- supported fixed dental prostheses (FDPs)? A systematic review of the survival and complication rates. Part I: single crowns (SCs)" [dental materials 31 (6) (2015) 603-623]. *Dent Mater*. 2016;*32*(12):e389-e390.
10. Sailer I, Strasding M, Valente NA, Zwahlen M, Liu S, Pjetursson BE. A systematic review of the survival and complication rates of zirconia-ceramic and metal-ceramic multiple-unit fixed dental prostheses. *Clin Oral Implants Res*. 2018;*29*(16):184-198.
11. Guess PC, Schultheis S, Bonfante EA, Coelho PG, Ferencz JL, Silva NR. All-ceramic systems: laboratory and clinical performance. *Dent Clin N Am*. 2011;*55*(2):333-352.
12. Sailer I, Balmer M, Husler J, Hammerle CHF, Kanel S, Thoma DS. 10-year randomized trial (RCT) of zirconia-ceramic and metal-ceramic fixed dental prostheses. *J Dent*. 2018;*76*:32-39.
13. Pieralli S, Kohal RJ, Jung RE, Vach K, Spies BC. Clinical outcomes of zirconia dental implants: a systematic review. *J Dent Res*. 2017;*96*(1):38-46.
14. Pjetursson BE, Zarauz C, Strasding M, Sailer I, Zwahlen M, Zembic A. A systematic review of the influence of the implant-abutment connection on the clinical outcomes of ceramic and metal implant abutments supporting fixed implant reconstructions. *Clin Oral Implants Res*. 2018;*29*(18):160-183.
15. Roehling S, Woelfler H, Hicklin S, Kniha H, Gahlert M. A retrospective clinical study with regard to survival and success rates of zirconia implants up to and after 7 years of loading. *Clin Implant Dent Relat Res*. 2016;*18*(3):545-558.
16. Sailer I, Philipp A, Zembic A, Pjetursson BE, Hammerle CH, Zwahlen M. A systematic review of the performance of ceramic and metal implant abutments supporting fixed implant reconstructions. *Clin Oral Implants Res*. 2009;*20*(4):4-31.

17. Hashim D, Cionca N, Courvoisier DS, Mombelli A. A systematic review of the clinical survival of zirconia implants. *Clin Oral Investig*. 2016;*20*(7):1403-1417.
18. Chevalier J, Cales B, Drouin JM. Low-temperature aging of Y-TZP ceramics. *J Am Ceram Soc*. 1999;*82*(8):2150-2154.
19. Kobayashi K, Kuwajima H, Masaki T. Phase change and mechanical properties of ZrO2-Y2O3 solid electrolyte after ageing. *Solid State Ion*. 1981;*3*:489-493.
20. Benalcazar Jalkh EB, Monteiro KN, Cesar PF, et al. Aging resistant ZTA composite for dental applications: microstructural, optical and mechanical characterization. *Dent Mater*. 2020;*36*(9):1190-1200.
21. Miragaya LM, Guimarães RB, Souza ROA, GDS B, JGA G, EMDS S. Effect of intra-oral aging on t→m phase transformation, microstructure, and mechanical properties of Y-TZP dental ceramics. *J Mech Behav Biomed Mater*. 2017;*72*:14-21.
22. Pezzotti G, Zhu W, Zanocco M, et al. Reconciling in vivo and in vitro kinetics of the polymorphic transformation in zirconia-toughened alumina for hip joints: II. Theory. *Korean J Couns Psychother*. 2017;*71*:446-451.
23. Schubert H, Frey F. Stability of Y-TZP during hydrothermal treatment: neutron experiments and stability considerations. *J Eur Ceram Soc*. 2005;*25*(9):1597-1602.
24. Benalcazar Jalkh EB, Bergamo ETP, Monteiro KN, et al. Others. Aging resistance of an experimental zirconia-toughened alumina composite for large span dental prostheses: optical and mechanical characterization. *J Mech Behav Biomed Mater*. 2020;*104*:103659.
25. Kim HK, Kim SH. Effect of hydrothermal aging on the optical properties of precolored dental monolithic zirconia ceramics. *J Prosthet Dent*. 2018;*121*(4):676-682.
26. Schneider JB, Kriegel S, Kaps R, Glien C, Oberbachy, T W. Low-temperature aging behavior of alumina-toughened zirconia. *J Am Ceram Soc*. 2008;*11*:3613-3618.
27. Sequeira S, Fernandes MH, Neves N, Almeida MM. Development and characterization of zirconia-alumina composites for orthopedic implants. *Ceram Int*. 2016;*43*(1):693-703.
28. Zhao YJ, Liao L, Wang Y, Lu C, Zhang J, Li J. Low temperature degradation of alumina toughened zirconia in artificial saliva. *J Wuhan Univ Technol Mater Sci Ed*. 2013;*28*(4):844-848.
29. Pereira GK, Venturini AB, Silvestri T, et al. Low-temperature degradation of Y-TZP ceramics: a systematic review and meta-analysis. *J Mech Behav Biomed Mater*. 2015;*55*:151-163.
30. Toraya H, Yoshimura M, Sōmiya S. Quantitative analysis of monoclinic-stabilized cubic ZrO2 systems by X-ray diffraction. *J Am Ceram Soc*. 1984;*67*:183-184.
31. Prado P, Monteiro JB, Campos TMB, Thim GP, de Melo RM. Degradation kinetics of high-translucency dental zirconias: mechanical properties and in-depth analysis of phase transformation. *J Mech Behav Biomed Mater*. 2019;*102*:103482.
32. Ceglias RB, Alves JM, Botelho RA, et al. Residual stress evaluation by X-ray diffraction and hole-drilling in an API 5L X70 steel pipe bent by hot induction. *Mater Res*. 2016;*19*:1176-1179.
33. Committee CT. *Colorimetry*. Vienna, Austria: CIE Central Bureau; 2004 CIE pub no 15.3.
34. Zhang F, Vanmeensel K, Inokoshi M, et al. Critical influence of alumina content on the low temperature degradation of 2–3 mol% yttria-stabilized TZP for dental restorations. *J Eur Ceram Soc*. 2015;*35*(2):741-750.
35. Camposilvan E, Leone R, Gremillard L, et al. Aging resistance, mechanical properties and translucency of different yttria-stabilized zirconia ceramics for monolithic dental crown applications. *Dent Mater*. 2018;*34*(6):879-890.
36. Becher PF, Swain MV. Grain-size-dependent transformation behavior in polycrystalline tetragonal zirconia. *J Am Ceram Soc*. 1992;*75*(3):493-502.
37. Krell AH, Klimke T. Transparent ceramics for structural applications: part 1 physics of light transmission and technological consequences. *Ceram Forum Int*. 2007;*84*(4):41-50.
38. Pekkan G, Pekkan K, Bayindir BC, Ozcan M, Karasu B. Factors affecting the translucency of monolithic zirconia ceramics: a review from materials science perspective. *Dent Mater J*. 2019;*39*(1):1-8.
39. Zhang Y. Making yttria-stabilized tetragonal zirconia translucent. *Dent Mater*. 2014;*30*(10):1195-1203.
40. Papageorgiou-Kyrana K, Fasoula M, Kontonasaki E. Translucency of monolithic zirconia after hydrothermal aging: a review of in vitro studies. *J Prosthodont*. 2020;*29*:489-500.
41. Ahmed WM, Troczynski T, McCullagh AP, Wyatt CCL, Carvalho RM. The influence of altering sintering protocols on the optical and mechanical properties of zirconia: a review. *J Esthet Restor Dent*. 2019;*31*(5):423-430.
42. Keuper M, Berthold C, Nickel KG. Long-time aging in 3 mol% yttria-stabilized tetragonal zirconia polycrystals at human body temperature. *Acta Biomater*. 2014;*10*(2):951-959.
43. Nishihara H, Haro Adanez M, Att W. Current status of zirconia implants in dentistry: preclinical tests. *J Prosthodont Res*. 2019;*63*(1):1-14.

How to cite this article: Bergamo ETP, Cardoso KB, Lino LFO, et al. Alumina-toughened zirconia for dental applications: Physicochemical, mechanical, optical, and residual stress characterization after artificial aging. *J Biomed Mater Res*. 2021;109:1135–1144. https://doi.org/10.1002/jbm.b.34776